Applied Energy Symposium 2022: Clean Energy towards Carbon Neutrality (CEN2022)
April 23-25, 2022, Ningbo, China
Paper ID: 0114

MOF-derived CoS_x and microspherical $ZnIn_2S_4$ with enhanced photocatalytic hydrogeneration activity

Yueying Zheng[a,b], Fan Wang[a,b], Yipei Chen[a,b], Tao Wu[a,b,c*]

a, New Materials Institute, University of Nottingham, Ningbo 315100, China

b, Department of Chemical and Environmental Engineering, University of Nottingham Ningbo China, Ningbo 315100, China

c, Key Laboratory of Carbonaceous Wastes Processing and Process Intensification of Zhejiang Province, Ningbo 315100, China

**Corresponding author: Tao Wu (tao.wu@nottingham.edu.cn)*

ABSTRACT

The design and preparation of highly effective semiconductor-based photocatalysts is an important issue for water splitting hydrogen generation. Based on design principle of Z-scheme heterojunction, a novel $ZnIn_2S_4/CoS_x$ photocatalyst for efficient carrier separation and transition is developed. The $ZnIn_2S_4$ exhibits a 3D flower-like microsphere structure, and ZIF-67-derived dodecahedral CoS_x nanospheres are tightly embedded in the $ZnIn_2S_4$ petals' gaps. This design allows for fast charge separation and transfer improving the hydrogen generation reaction efficiency considerably. The $ZnIn_2S_4/CoS_x$ heterostructure photocatalyst has high photoactivity under visible light irradiation with a hydrogen-producing rate of more than 8 mmol g^{-1} h^{-1}, which is about 6-fold of the pristine $ZnIn_2S_4$.

Keywords: MOF, Dodecahedral CoS_x, $ZnIn_2S_4$, hydrogen generation

1. INTRODUCTION

Semiconductor photocatalysis of water splitting for hydrogen production is considered as an effective alternative energy technology in solving global energy crisis[1]. It utilizes plentiful sunlight to produce renewable H_2 as an energy source.[2, 3]. Photocatalytic hydrogen production has the advantages of simplicity, rapidity, low cost, less pollution, and direct use of water as raw material[4-7]. For these advantages to be fully realized, a logical design of high-efficient and stable photocatalysts is particularly essential. Therefore, it is imperative to develop a novel semiconductor photocatalyst with excellent photocatalytic properties and construct an efficient and low-cost visible-light-responsive photocatalytic system.

Due to its favorable and adjustable band gap of 2-3 eV, and conduction band position for water reduction, $ZnIn_2S_4$ has been considered as a general excellent option for solar hydrogen production[8-11]. Nevertheless, Individual $ZnIn_2S_4$ photocatalytic properties are insufficient due to the substantial recombination of the carriers and its main absorption light region outside desired visible light[12]. Thus, heterostructure are frequently utilized to makes for its deficiency. Furthermore, metal organic frameworks (MOFs) and its derivatives have been used to catalyze various reactions due to its regular morphology and the multiple active sites by its large surface area and hierarchical porous structure[13-15]. MOFs can be calcinated to form regular structure oxidates, which are also common hydrogen generation photocatalysts[16]. In this work, an after-treated ZIF-67 formed a special dodecahedral structure of CoS_x that partially retains the structure of ZIF-67. Construction of heterojunctions composite materials made by varying energy band is a common method to boost the photocatalytic performance[17, 18]. In particular, direct Z-scheme heterostructure is one of the most desired structures, having the most efficient electron transfer routes[19]. The principle of designing Z-scheme heterostructure is matching the CB and VB of two composite materials close enough enabling electrons transports along the Z-scheme pathway[20].

In this paper, the Z-Scheme heterojunction formed by $ZnIn_2S_4$ and CoS_x has a great improvement in hydrogen production efficiency compared with single $ZnIn_2S_4$ and

Selection and peer-review under the responsibility of the scientific committee of the CEN2022.

CoS_x since the Z-Scheme heterostructure developed by Bard et al. has the benefits of excellent photo-excited hole-electron pair separation ability[18]. The optimal hydrogen production ratio was found by adjusting different ratios of CoS_x on $ZnIn_2S_4$, and the mechanism was analyzed.

2. EXPERIMENT

2.1 Material and methods

$ZnIn_2S_4$ and ZIF-67 was synthesized by a modified hydrothermal method respectively[16, 21, 22]. The obtained ZIF-67 was further reacted with sulfur source in the autoclave at 180 °C for 3h, and the solid obtained was washed and collected, noted as CoS_x. It was further combined with $ZnIn_2S_4$ under ultrasonic heating conditions for 5h to form $ZnIn_2S_4/CoS_x$ heterostructure.

2.2 Results and Discussion

As shown in Fig. 1(a), the uniform and regular dodecahedral CoS_x nanostructure with a diameter of approximately 500nm was generated from the dodecahedral precursor ZIF-67. Fig. 1(b-d) shows the morphology of $CoS_x/Znin_2S_4$ composite. The average particle size of spherical $ZnIn_2S_4$ with petal surface is 4μm. CoS_x nanoparticles are evenly distributed on the petal folds surface of spherical structure. It can be seen from the figure that the combination of two components is close and the combination area is large, forming a stable composite structure, which is conducive to photoelectron migration between the structures. To determine the proportion of the two components in the complex, EDS was used to scan the elemental mass ratio, as shown in Fig. 2.It can be concluded by calculation that CoS_x is loaded on the surface of spherical $ZnIn_2S_4$ at a ratio of approximately 10wt%, which is coincide with expectations.

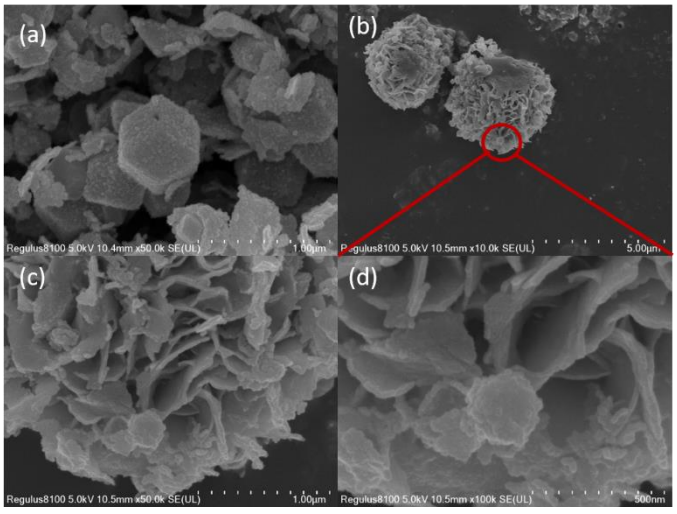

Fig. 1. SEM images of a) CoS_x nanoparticles, b), c), d) $ZnIn_2S_4/CoS_x$ at different magnifications

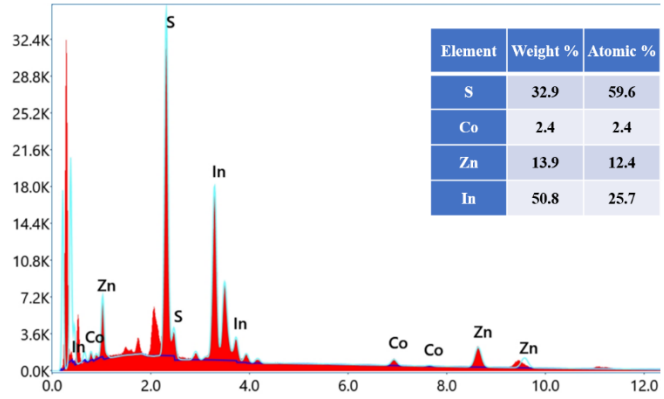

Fig. 2. EDS mapping of $ZnIn_2S_4/CoS_x$

XRD patterns in Fig. 3 gives that the main characteristic peaks of the synthesized materials are high and narrow, which proves that the materials have high crystallinity and purity. $ZnIn_2S_4$ can be indexed as JCPDS PDF#89-3963 shown in figure, in which $ZnIn_2S_4$ is a spherical structure with petal-like surface, consistent with the SEM results of the synthesized samples. Compared with the standard index, three main peaks of pure $ZnIn_2S_4$ could be observed at 21.586°, 27.691° and 47.175°, corresponding to the facets (0 0 6), (1 0 2) and (1 1 0), respectively.

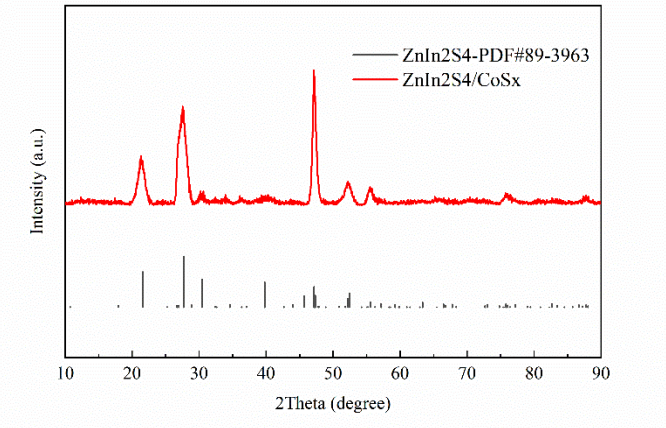

Fig. 3 XRD patterns of $ZnIn_2S_4/CoS_x$ and JCPDS NO#89-3963 of $ZnIn_2S_4$

Fig. 4 is the photoluminescence spectra (PL) illustrating the rate of photoexited pairs recombination. The more intense the PL spectrum, the higher the recombination rate of photo-generated pairs, and consequently the lower the photocatalytic activity is. As

is observed that CoS_x and $ZnIn_2S_4$ both have an intense emission peak, it indicates a strong recombination of photo-generated carriers inside them; while the emission peak intensity of $ZnIn_2S_4/CoS_x$ is much lower compared with them, implying the heterostructure composite develop the water splitting activity by inhibiting photocarrier recombination in the system.

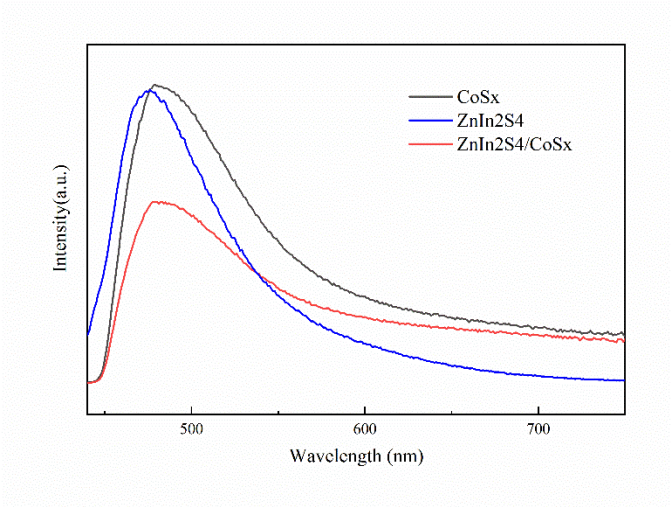

Fig. 4. Photoluminescence (PL) spectra of CoS_x, $ZnIn_2S_4$ and $ZnIn2S_4/CoS_x$

The photocatalytic water splitting performance of materials was investigated under visible light irradiation (420 nm) and using triethanolamine (TEOA) as a hole scavenger. As is proved by the control trials that there is no detectable H2 production without irradiation, H_2 is produced by photocatalytic conditions. Fig. 5 displays the hydrogen generation rates of samples, in which the $ZnIn_2S_4$ particles having an H_2 evolution rate of 1.4193 mmol h^{-1} g^{-1}. It is clear that when $ZnIn_2S_4$ is combined with CoS_x, the composites exhibit significantly increased activity, with the greatest rate of 8.0441 mmol h^{-1} g^{-1}, indicating that the heterostructure has a significant positive effect on the photocatalytic activity. This rate of H_2 production in absence of noble metals is competitive to that described in previous publications[23]. This study indicates the photocatalytic benefit of the composite heterostructure. The bare CoS_x sample is essentially inert, most likely due to the fast frequency of photoexcited charge recombination and undesirable band gap. The $ZnIn_2S_4/CoS_x$ composite is also tested to be robust in terms of H_2 generation over a long cyclic time. These findings reveal the better water splitting photocatalytic hydrogen generation performance of $ZnIn_2S_4/CoS_x$, which is supported by the heterostructures that allow for effective separation and transfer of charge carriers.

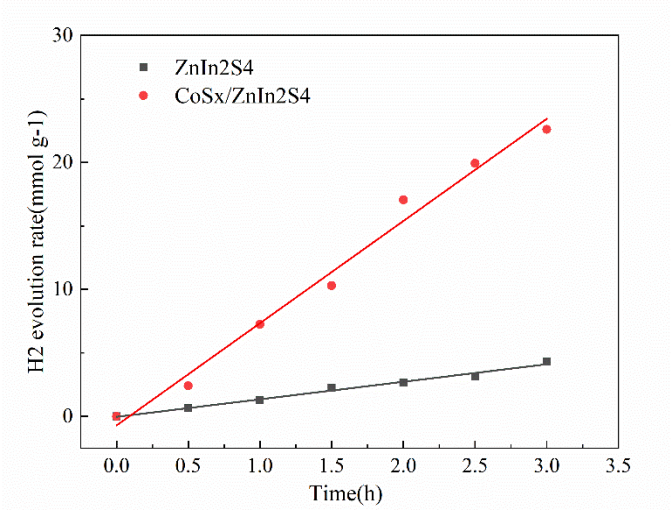

Fig. 5. H_2 generation rate with time by $ZnIn_2S_4$ and $ZnIn_2S_4/CoS_x$ under visible light

As represented in Fig. 6, the UV-vis DRS spectra from 200 to 900 nm were measured, reflecting the capability of photocatalysts in absorbing light by respectively wave range and intensity. CoS_x exhibits substantial absorption in the whole light range, while the absorption edge of $ZnIn_2S_4$ is at about 550 nm. The $ZnIn_2S_4/CoS_x$ shows an improved light absorption combining the benefits from two material, which contributes to the improvement of the photocatalytic efficiency.

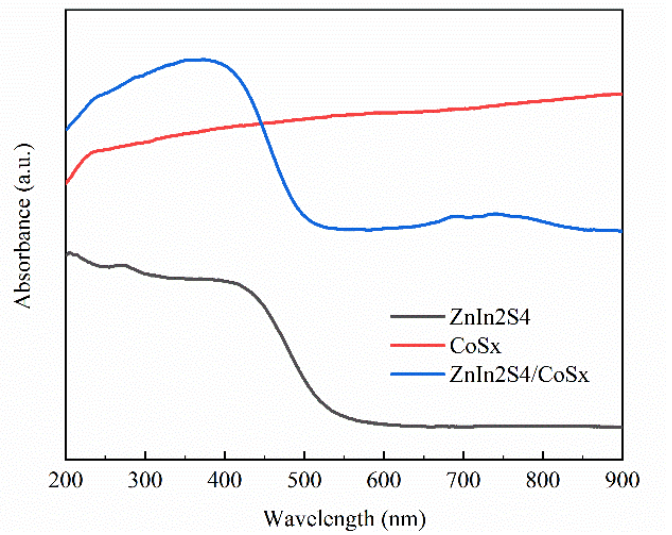

Fig. 6. UV-vis DRS spectra of CoS_x, $ZnIn_2S_4$ and $ZnIn2S_4/CoS_x$

Tauc plots derived from UV-vis DRS results were calculated shown in Fig. 7. The Kubelka-Munk formula $(ahv)^{1/n} = A(hv-Eg)$ was used[24, 25], and the band gap of $ZnIn2S_4$ and CoS_x was respectively calculated to be 2.46 eV and 1.00 eV, which agrees with the results that have been published[26, 27]

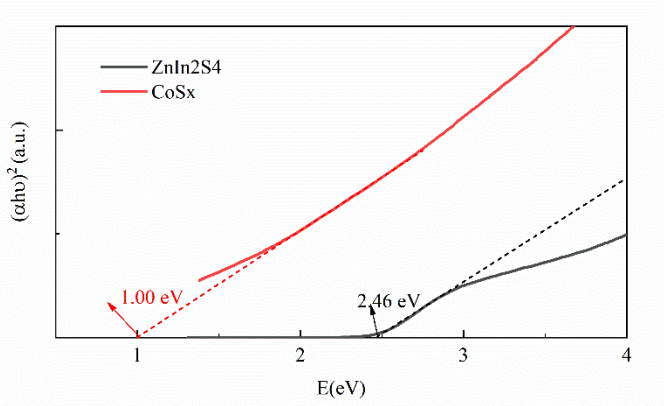

Fig. 7. Tauc plot of $ZnIn2S_4$ and CoS_x

Fig. 8 displays the valence band X-ray photoelectron spectroscopy (VB XPS) spectra of $ZnIn2S_4$ and CoS_x, which gives that the VB positions of $ZnIn2S_4$ and CoS_x are 1.52 eV and -0.10 eV, according to the formula: $E_{VB,\ NHE} = \phi + E_{VB,XPS} - 4.44$, where ϕ is the work function[7]. Furthermore, the CB of $ZnIn_2S_4$ and CoS_x can be computed to be -0.94 and -1.10 eV respectively, by the formula: $E_{CB}=E_{VB}-E_g$ using the energy band gap from UV-vis DRS results calculated above.

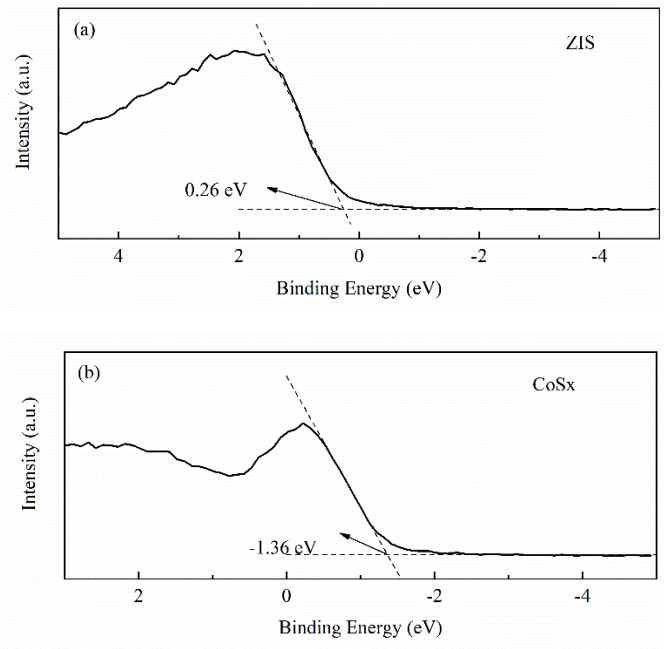

Fig. 8. XPS VB spectra of (a) $ZnIn2S_4$ and (b) CoS_x

As seen in Figure 9, the strong interface between $ZnIn_2S_4$ and CoS_x works as an effective photoexcited electron transfer route from the conduction band of $ZnIn_2S_4$ to the valence band of CoS_x, which functions to separate the hole and electron acceptor center. The electrons produced on CoS_x were further caught by H^+ in water and the reduction process happens, generating H_2. By transferring electrons from $ZnIn2S_4$ to CoS_x over the long-distance interface, the electron-hole pair recombination is reduced by the long transition pathway and energy barrier, and thus the photocatalytic activity is promoted.

For the oxidation side, the sacrificial reagents capture the holes generated by $ZnIn_2S_4$ rapidly.

This Z-scheme heterostructure photocatalyst with high hydrogen generation capability and non-metal component offers a promising development for solving energy concerns by sustainable and economical photocatalysis.

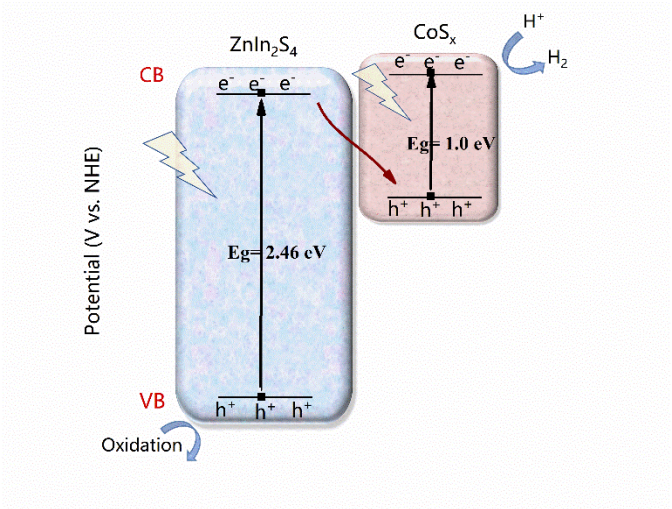

Fig. 9. Band structure schematic illustration of charge transfer mechanism of $ZnIn_2S_4/CoS_x$

2.3 Conclusions

A novel Z-Scheme heterostructure $ZnIn_2S_4/CoS_x$ photocatalyst has been synthesized with controlled regular morphology derived from MOF structure pattern. This heterostructures promotes light absorption ability as well as carrier separation and transport efficiency of photocatalysts. Under visible light irradiation, this photocatalyst demonstrates considerably high photocatalytic H_2 evolution activity. This finding provides insights on designing efficient heterostructure semiconductor photocatalysts.

ACKNOWLEDGEMENT

This work was supported by the Provincial Key Laboratory Programme of Zhejiang Provincial Department of Science and Technology (grant number 2020E10018) and Municipal Engineering Centre for Carbonaceous Solid Waste Processing and Process Intensification.

REFERENCE

1. Rafique, M., et al., *A Comprehensive Study on Methods and Materials for Photocatalytic Water Splitting and Hydrogen Production as a Renewable Energy Resource.* Journal of Inorganic and Organometallic Polymers and Materials, 2020. **30**(10): p. 3837-3861.
2. Abanades, *Metal Oxides Applied to Thermochemical Water-Splitting for Hydrogen Production Using Concentrated Solar Energy.* ChemEngineering, 2019. **3**(3).
3. Hosseini, S.E. and M.A. Wahid, *Hydrogen from solar energy, a clean energy carrier from a sustainable source of energy.* International Journal of Energy Research, 2020. **44**(6): p. 4110-4131.
4. Kim, D. and K. Yong, *Boron doping induced charge transfer switching of a C3N4/ZnO photocatalyst from Z-scheme to type II to enhance photocatalytic hydrogen production.* Applied Catalysis B: Environmental, 2021. **282**.
5. Liu, Y., Z. Sun, and Y.H. Hu, *Bimetallic cocatalysts for photocatalytic hydrogen production from water.* Chemical Engineering Journal, 2021. **409**.
6. Yang, Y., et al., *Recent advances in application of transition metal phosphides for photocatalytic hydrogen production.* Chemical Engineering Journal, 2021. **405**.
7. Ran, J., et al., *Significantly Raised Visible-Light Photocatalytic H2 Evolution on a 2D/2D ReS2/In2ZnS4 van der Waals Heterostructure.* Small, 2021. **n/a**(n/a): p. 2100296.
8. Wang, M., et al., *Spatially Separating Redox Centers and Photothermal Effect Synergistically Boosting the Photocatalytic Hydrogen Evolution of ZnIn2 S4 Nanosheets.* Small, 2021. **17**(17): p. e2006952.
9. Wang, X., et al., *Interfacial chemical bond and internal electric field modulated Z-scheme Sv-ZnIn2S4/MoSe2 photocatalyst for efficient hydrogen evolution.* Nat Commun, 2021. **12**(1): p. 4112.
10. Zhang, S., et al., *Gradient Hydrogen Migration Modulated with Self-Adapting S Vacancy in Copper-Doped ZnIn2S4 Nanosheet for Photocatalytic Hydrogen Evolution.* ACS Nano, 2021. **15**(9): p. 15238-15248.
11. Chandrasekaran, S., et al., *Recent advances in metal sulfides: from controlled fabrication to electrocatalytic, photocatalytic and photoelectrochemical water splitting and beyond.* Chemical Society Reviews, 2019. **48**(15): p. 4178-4280.
12. Wang, X., et al., *Interfacial chemical bond and internal electric field modulated Z-scheme Sv-ZnIn2S4/MoSe2 photocatalyst for efficient hydrogen evolution.* Nature Communications, 2021. **12**(1): p. 4112.
13. Bhadra, B.N., et al., *MOF-derived carbonaceous materials enriched with nitrogen: Preparation and applications in adsorption and catalysis.* Materials Today, 2019. **25**: p. 88-111.
14. Wang, Z., et al., *Nickel-based cocatalysts for photocatalysis: Hydrogen evolution, overall water splitting and CO2 reduction.* Materials Today Physics, 2020. **15**.
15. Xia, B., et al., *Photocatalysts for Hydrogen Evolution Coupled with Production of Value‐Added Chemicals.* Small Methods, 2020. **4**(7).
16. Zhang, L., Z. Jin, and N. Tsubaki, *Zeolitic Imidazolate Framework-67-Derived P-Doped Hollow Porous Co3O4 as a Photocatalyst for Hydrogen Production from Water.* ACS Applied Materials & Interfaces, 2021.
17. Zhong, Y., et al., *Interface engineering of heterojunction photocatalysts based on 1D nanomaterials.* Catalysis Science & Technology, 2021. **11**(1): p. 27-42.
18. Bard, A.J., *Photoelectrochemistry and heterogeneous photo-catalysis at semiconductors.* Journal of Photochemistry, 1979. **10**(1): p. 59-75.
19. Low, J., et al., *Heterojunction Photocatalysts.* Advanced Materials, 2017. **29**(20): p. 1601694.
20. Li, J. and N. Wu, *Semiconductor-based photocatalysts and photoelectrochemical cells for solar fuel generation: a review.* Catalysis Science & Technology, 2015. **5**(3): p. 1360-1384.
21. Wang, S., et al., *Formation of Hierarchical Co9S8@ZnIn2S4 Heterostructured Cages as an Efficient Photocatalyst for Hydrogen Evolution.* J Am Chem Soc, 2018. **140**(45): p. 15145-15148.
22. Wu, Y., et al., *Effects of composition faults in ternary metal chalcogenides (ZnxIn2S3+x, x = 1–5) layered crystals for visible-light-driven catalytic hydrogen generation and carbon dioxide reduction.* Applied Catalysis B: Environmental, 2019. **256**: p. 117810.
23. Li, Y., et al., *Oriented ZnmIn2Sm+3@In2S3 heterojunction with hierarchical structure for efficient photocatalytic hydrogen evolution.* Applied Catalysis B: Environmental, 2019. **244**: p. 604-611.
24. Murugalakshmi, M., G. Mamba, and V. Muthuraj, *A novel In2S3/Gd2O3 p-n type visible light-driven heterojunction photocatalyst for dual role of Cr(VI) reduction and oxytetracycline degradation.* Applied Surface Science, 2020. **527**: p. 146890.
25. Wenderich, K. and G. Mul, *Methods, Mechanism, and Applications of Photodeposition in Photocatalysis: A Review.* Chemical Reviews, 2016. **116**(23): p. 14587-14619.
26. Ding, Y., et al., *Rational design of Z-scheme PtS-ZnIn2S4/WO3-MnO2 for overall photo-catalytic water splitting under visible light.* Applied Catalysis B: Environmental, 2019. **258**: p. 117948.
27. Carević, M.V., et al., *Formation of ZnIn2S4 nanosheets and tubular structures in organic media.* Materials Research Bulletin, 2017. **87**: p. 140-147.